

# Revisiting Entropy in Reinforcement Learning for Large Reasoning Models

Renren Jin<sup>1</sup>, Pengzhi Gao<sup>2</sup>, Yuqi Ren<sup>1</sup>, Zhuowen Han<sup>1</sup>, Tongxuan Zhang<sup>3</sup>  
 Wuwei Huang<sup>2</sup>, Wei Liu<sup>2</sup>, Jian Luan<sup>2</sup>, Deyi Xiong<sup>1\*</sup>

<sup>1</sup>School of Computer Science and Technology, Tianjin University

<sup>2</sup>Unaffiliated

<sup>3</sup>College of Computer and Information Engineering, Tianjin Normal University

{rrjin, dyxiong}@tju.edu.cn

## Abstract

Reinforcement learning with verifiable rewards (RLVR) has emerged as a predominant approach for enhancing the reasoning capabilities of large language models (LLMs). However, the entropy of LLMs usually collapses during RLVR training, causing premature convergence to suboptimal local minima and hinder further performance improvement. Although various approaches have been proposed to mitigate entropy collapse, a comprehensive study of entropy in RLVR remains lacking. To address this gap, we conduct extensive experiments to investigate the entropy dynamics of LLMs trained with RLVR and analyze how model entropy correlates with response diversity, calibration, and performance across various benchmarks. Our findings reveal that the number of off-policy updates, the diversity of training data, and the clipping thresholds in the optimization objective are critical factors influencing the entropy of LLMs trained with RLVR. Moreover, we theoretically and empirically demonstrate that tokens with positive advantages are the primary contributors to entropy collapse, and that model entropy can be effectively regulated by adjusting the relative loss weights of tokens with positive and negative advantages during training.

## 1 Introduction

Pioneered by OpenAI o1 (Jaech et al., 2024), DeepSeek-R1 (DeepSeek-AI et al., 2025), and Kimi k1.5 (DeepSeek-AI et al., 2025), reinforcement learning with verifiable rewards (RLVR) has been widely employed to extend the boundaries of reasoning capacity in large language models (LLMs). LLMs trained with RLVR have demonstrated remarkable performance on tasks requiring sophisticated reasoning processes, such as mathematics and coding (Ye et al., 2025; Liu et al., 2025b; Luo et al., 2025; He et al., 2025).

However, although RLVR enhances the reasoning ability of LLMs, a growing body of research has shown that it can also drive LLMs toward entropy collapse, wherein the entropy of the model decreases substantially during training, ultimately reaching a markedly low level (Yu et al., 2025; Li et al., 2025a). Entropy collapse indicates that the probability mass over the model’s vocabulary becomes concentrated on a limited subset of tokens. This phenomenon further implies that LLMs increasingly prioritize exploitation over exploration. As a result, they fail to effectively explore novel reasoning paths during training, thereby potentially causing premature convergence to a local optimum.

To address entropy collapse in LLMs, numerous methods have been proposed. Shen (2025) and He et al. (2025) incorporate an entropy maximization term into the RLVR objective. DAPO (Yu et al., 2025) raises the upper clipping bound of the importance ratio to avoid clipping low-probability tokens. Cui et al. (2025) restrict parameter updates for tokens with high covariance between log-probability and advantage, alongside other approaches (Wang et al., 2025b; Chen et al., 2025; Deng et al., 2025; Li et al., 2025a; Zhu et al., 2025). Despite these advances, systematic investigations of entropy in RLVR remain scarce. Specifically, three critical questions are still underexplored: (1) How does the entropy of LLMs trained with RLVR correlate with their performance? (2) What factors govern entropy dynamics, both theoretically and empirically? and (3) How can entropy be effectively regulated to improve the performance of LLMs?

To investigate the above research questions, we conduct extensive experiments on RLVR. The results show that the entropy of LLMs trained with RLVR is strongly correlated with response diversity, as LLMs with lower entropy tend to produce less diverse outputs. During training, both response and prompt entropy consistently decline, with in-domain prompts decreasing more rapidly than out-

\* Corresponding author.

of-domain ones. However, prompt entropy shows only a weak correlation with the accuracy of corresponding responses. Moreover, we observe that model performance can continue to improve even without a reduction in entropy. Entropy also proves to be an unreliable indicator of model performance across most benchmarks, as the correlations between entropy and performance are task-dependent. Empirically, we find that entropy collapse is associated with model miscalibration, and that more severe entropy collapse corresponds to stronger miscalibration. Beyond these findings, we identify three key factors that influence entropy dynamics: (1) the number of off-policy updates, (2) training data diversity, and (3) the clipping threshold. Surprisingly, LLMs trained on approximately 600 samples achieve performance comparable to those trained on about 17k samples. Finally, we theoretically and empirically demonstrate that tokens with positive advantages are the primary contributors to entropy collapse. Adjusting the relative loss weights assigned to tokens with positive and negative advantages effectively regulates entropy and improves LLM performance on benchmarks. Our contributions can be summarized as follows:

- We conduct extensive experiments to investigate the entropy dynamics of LLMs trained with RLVR, revealing how entropy interacts with response diversity, calibration, and performance on various benchmarks.
- We identify three key factors influencing the entropy dynamics of LLMs during RLVR training: (1) off-policy updates, (2) training data diversity, and (3) clipping threshold.
- We theoretically and empirically demonstrate that entropy collapse in RLVR primarily arises from tokens with positive advantages, and that regulating their relative loss weights provides an effective means to control entropy and improve model performance.

## 2 Related Work

Entropy has long served as a regularization mechanism to encourage exploration in reinforcement learning (Ziebart et al., 2008; Ziebart, 2010). In the era of LLMs, several studies have similarly incorporated entropy maximization objectives into RLVR to promote exploration and prevent premature convergence (Shen, 2025; He et al., 2025). Aiming to mitigate entropy collapse, Clip-Higher

(Yu et al., 2025) raises the upper clipping bound of the importance ratio to prevent low-probability tokens with positive advantages from being clipped. Liu (2025) and Cui et al. (2025) provide theoretical insights into entropy dynamics, showing that tokens with strong positive covariance between their probabilities and corresponding advantages primarily drive entropy collapse. Building on these insights, Clip-Cov and KL-Cov (Cui et al., 2025) limit updates on tokens exhibiting such covariance. Similarly, CE-GPPO (Su et al., 2025) mitigates entropy collapse by preserving the gradients of clipped tokens through a stop-gradient operation. Furthermore, Wang et al. (2025b) train LLMs using only high-entropy tokens to enhance model performance, while Cheng et al. (2025) incorporate entropy terms into the advantage to encourage exploration and improve reasoning capabilities. Numerous other studies have also explored entropy-based mechanisms to further enhance the performance of LLMs trained with RLVR (Li et al., 2025a; Wang et al., 2025a; Liu et al., 2025a).

## 3 Preliminaries

### 3.1 Group Relative Policy Optimization (GRPO)

Let the prompt be  $\mathbf{x}$  and the response generated by the LLM  $\pi_\theta$  (parameterized by  $\theta$ ) be  $\mathbf{y}$ . The reward for response  $\mathbf{y}$  is denoted as  $R(\mathbf{y})$ . The RLVR objective is to maximize the expected reward of responses generated by  $\pi_\theta$ , formulated as:

$$J(\theta) = \mathbb{E}_{\mathbf{y} \sim \pi_\theta(\cdot | \mathbf{x})} R(\mathbf{y}). \quad (1)$$

To optimize  $\pi_\theta$  for maximizing the expected reward, GRPO (Shao et al., 2024) adopts the surrogate objective of PPO (Schulman et al., 2017), replacing critic-based advantage estimation with group-based reward normalization to reduce the memory and computational cost of training a critic. Instead of learning a state-value function, GRPO samples multiple responses per prompt and computes each response’s advantage by normalizing its reward with the group’s mean and standard deviation. Following DAPO, we employ a token-level loss to ensure equal token contribution across responses of varying lengths and remove the KL penalty term from the original GRPO objective. Formally, let  $\pi_\theta$  sample  $G$  responses  $\{\mathbf{y}^j\}_{j=1}^G$  for each prompt  $\mathbf{x}$ , and let  $\mathcal{D}$  denote the prompt dataset. The optimization objective of GRPO with token-

level loss and without the KL penalty term is:

$$\begin{aligned} \mathcal{J}(\theta) = & \mathbb{E}_{\mathbf{x} \sim \mathcal{D}, \{\mathbf{y}^i\}_{i=1}^G \sim \pi_{\theta_{\text{old}}}(\cdot | \mathbf{x})} \\ & \left[ \frac{1}{\sum_{i=1}^G |\mathbf{y}^i|} \sum_{i=1}^G \sum_{t=1}^{|\mathbf{y}^i|} \min \left( r_{i,t}(\theta) \hat{A}_{i,t}, \right. \right. \\ & \left. \left. \text{clip} (r_{i,t}(\theta), 1 - \varepsilon_{\text{low}}, 1 + \varepsilon_{\text{high}}) \hat{A}_{i,t} \right) \right], \end{aligned} \quad (2)$$

where  $r_{i,t}(\theta) = \frac{\pi_\theta(\mathbf{y}_t^i | \mathbf{x}, \mathbf{y}_{<t}^i)}{\pi_{\theta_{\text{old}}}(\mathbf{y}_t^i | \mathbf{x}, \mathbf{y}_{<t}^i)}$ , the advantage is given by  $\hat{A}_{i,t} = \frac{R(\mathbf{y}^i) - \text{mean}(\{R(\mathbf{y}^j)\}_{j=1}^G)}{\text{std}(\{R(\mathbf{y}^j)\}_{j=1}^G)}$ , and  $\varepsilon_{\text{low}}$  and  $\varepsilon_{\text{high}}$  are clipping hyperparameters controlling the lower and upper bounds, respectively.

### 3.2 Entropy Regularization

Let the vocabulary of  $\pi_\theta$  be denoted by  $\mathcal{V}$ . For a prompt  $\mathbf{x}$  and response  $\mathbf{y}$ , the token-level average entropy is defined as follows:

$$\mathcal{H}(\pi_\theta) = -\frac{1}{|\mathbf{y}|} \sum_{t=1}^{|\mathbf{y}|} \sum_{v \in \mathcal{V}} \pi_\theta(v | \mathbf{x}, \mathbf{y}_{<t}) \log \pi_\theta(v | \mathbf{x}, \mathbf{y}_{<t}). \quad (3)$$

Entropy regularization augments the RLVR objective with the term  $\alpha \mathcal{H}(\pi_\theta)$ , where  $\alpha$  is the entropy regularization coefficient.

#### 3.2.1 Adaptive Entropy Regularization

Despite the effectiveness of vanilla entropy regularization in controlling LLM entropy, prior studies have shown that selecting an appropriate regularization coefficient is challenging (He et al., 2025): a large coefficient causes entropy to rise rapidly, while a small one renders the regularization ineffective. To address this, He et al. (2025) propose adaptive entropy regularization, which dynamically adjusts the coefficient according to the model’s entropy rather than keeping it fixed during training. Let the entropy of the LLM  $\pi_\theta$  at training step  $k$  be denoted as  $\mathcal{H}_k(\pi_\theta)$ . The objective is to prevent the entropy from falling substantially below a pre-defined threshold  $\delta$ , and the entropy regularization coefficient at step  $k$ ,  $\alpha_k$ , is defined as follows:

$$\alpha_k = c_k \cdot \mathbb{I}\{\mathcal{H}_k(\pi_\theta) < \delta\}, \quad (4)$$

where the adaptive coefficient  $c_k$  is updated according to the following rule:

$$c_{k+1} = c_k + \beta \mathbb{I}\{\mathcal{H}_k(\pi_\theta) < \delta\} - \beta \mathbb{I}\{\mathcal{H}_k(\pi_\theta) \geq \delta\}. \quad (5)$$

Equation (4) indicates that entropy regularization is applied only when the entropy drops below the threshold  $\delta$ , setting the coefficient to  $c_k$ . Equation (5) defines the update rule: if the entropy is below  $\delta$ ,  $c_k$  increases by  $\beta$ ; otherwise, it decreases by  $\beta$ .

## 4 Experimental Setup

We trained Qwen2.5-Math-7B (Yang et al., 2024) with RLVR using the veRL framework (Sheng et al., 2025) on the DAPO-Math-17K dataset (Yu et al., 2025). Training employed a rollout batch size of 256, generating 16 responses per prompt. The AdamW optimizer was applied with a cosine learning rate schedule and a peak rate of  $1 \times 10^{-6}$ . During rollouts, decoding parameters were fixed as: top- $p = 1.0$ , temperature = 1.0, and a maximum generation length of 4096 tokens.

We evaluated both in-domain and out-of-domain performance. The in-domain benchmarks included AIME 2024/2025 (MAA, 2024, 2025), MATH500 (Hendrycks et al., 2021), AMC 2023 (MAA, 2023), and Minerva Math (Lewkowycz et al., 2022), while out-of-domain evaluation covered LiveCodeBench (Jain et al., 2025) for coding and IF-Eval (Zhou et al., 2023) for instruction following. For each question, we sampled 64 responses and reported Avg@64 and Pass@64. Evaluation was performed under two decoding settings: (1) temperature 1.0, top- $p$  1.0, and (2) temperature 0.6, top- $p$  0.95, both with a maximum length of 4096 tokens. To mitigate potential data contamination in the Qwen2.5 series of LLMs (Wu et al., 2025), AIME 2025 served as the validation set, and the best checkpoint was evaluated on all other benchmarks.

## 5 How Does the Entropy of LLMs Trained with RLVR Correlate with Their Performance?

### 5.1 Entropy and Response Diversity

The diversity of responses generated by LLMs is strongly positively correlated with both the entropy of these responses and the entropy of the LLMs during training.

To examine the relationship between response diversity and model entropy, we control LLM entropy using vanilla entropy regularization by varying the regularization coefficient. Experiments are conducted with coefficients  $\{0.001, 0.002\}$ , without entropy regularization, and with a negative coefficient  $-0.001$  that explicitly promotes entropy minimization. Response diversity is measured using the N-gram Diversity (Li et al., 2016) and SelfBLEU (Zhu et al., 2018) metrics. Formal definitions of these metrics are provided in Appendix A.

Figure 1 shows the entropy dynamics during

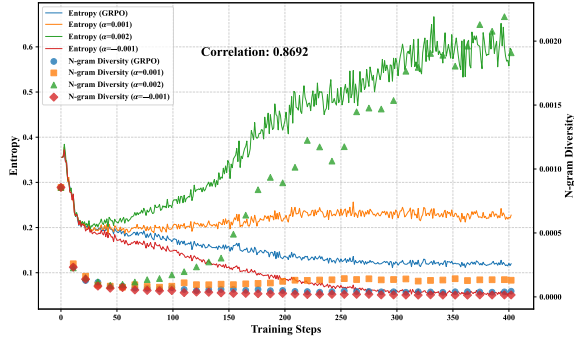


Figure 1: Evolution of entropy (solid lines) and N-gram diversity (markers) over training steps under different entropy regularization settings.

RLVR training alongside the N-gram Diversity of responses for AIME 2024 prompts. As shown in Figure 1, LLMs trained with GRPO exhibit entropy collapse during training, which is alleviated by vanilla entropy regularization with  $\alpha = 0.001$ , while a larger coefficient ( $\alpha = 0.002$ ) causes entropy to increase continuously in later stages. Conversely, applying a negative coefficient ( $\alpha = -0.001$ ) further exacerbates entropy collapse. Notably, N-gram Diversity follows a similar trajectory to entropy, with an average Pearson correlation of 0.8692 across the four training settings, indicating a strong positive correlation between response diversity and model entropy during training.

## 5.2 Entropy Dynamics on Prompts

During RLVR training, the entropy of LLMs decreases for both in-domain and out-of-domain prompts, with a more substantial reduction observed for in-domain prompts.

In addition to examining the entropy dynamics of responses generated by LLMs trained with RLVR, we also analyze the entropy dynamics of LLMs on prompts during RLVR training. Specifically, we compute the ratio between the entropy of LLMs on prompts at different training steps and their entropy on the same prompts before training, as shown in Figure 2. The entropy of LLMs on prompts decreases over training and eventually stabilizes. This reduction is more pronounced for prompts from the in-domain AIME 2024 benchmark than for those from the out-of-domain IF-Eval benchmark. Moreover, similar to preventing entropy collapse in generated responses, applying a positive entropy regularization coefficient helps maintain the entropy of LLMs on prompts.

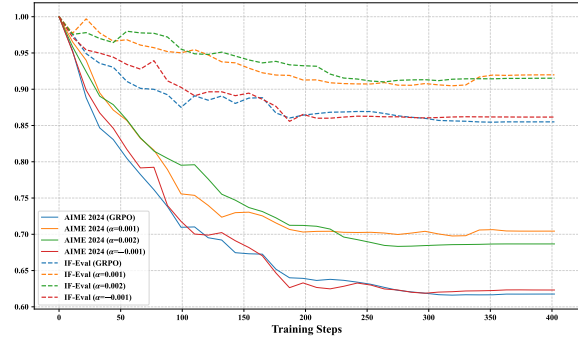


Figure 2: The ratio between the entropy of the LLMs on prompts during training and their entropy on the same prompts before training, plotted against training steps. Solid lines represent results on the AIME 2024, while dashed lines correspond to results on IF-Eval.

## 5.3 Prompt Entropy and Accuracy

The entropy of LLMs on prompts shows only a weak correlation with their accuracy.

To examine the correlation between the entropy of LLMs on prompts and their corresponding accuracy, we measure the accuracy of each prompt as the proportion of correct responses among 64 generated responses. Figure 3 presents the scatter plot of entropy versus accuracy across AIME 2024, AIME 2025, and MATH500 for Qwen2.5-Math-7B. The figure shows that the entropy of LLMs on prompts is only weakly correlated with accuracy, as evidenced by the small average Pearson correlation coefficient (0.1542) across the three benchmarks. We further compute the Pearson correlation coefficient between entropy and accuracy at different training steps. As shown in Figure 4, although the coefficient fluctuates throughout training, it remains consistently small, confirming the weak correlation between entropy and accuracy.

## 5.4 Performance Gains Without Trading Off Entropy

The performance of LLMs continues to improve during training, even as their entropy fluctuates around the value observed before training, indicating that performance gains are not solely achieved by trading off entropy.

To maintain the entropy of LLMs at a level comparable to that observed before training, we apply adaptive entropy regularization during RLVR training. Specifically, we randomly sample 1,000 prompts from the training dataset and compute

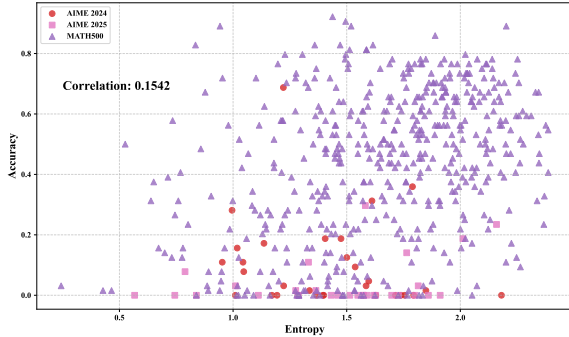


Figure 3: Scatter plot of accuracy versus entropy across AIME 2024, AIME 2025, and MATH500.

the entropy of the LLMs on the corresponding responses prior to training. The computed entropy value is then set as the predefined threshold  $\delta$ , ensuring that the entropy of the LLMs remains above this threshold throughout training.

Figure 6 illustrates the evolution of entropy and accuracy on AIME 2024. As shown in Figure 6, under adaptive entropy regularization, the entropy of LLMs decreases sharply at the beginning of training, then increases, and subsequently fluctuates around the specified threshold. Meanwhile, accuracy on AIME 2024 exhibits an upward trend, even surpassing that of the model trained without adaptive entropy regularization. This observation indicates that performance improvement of LLMs is not merely achieved by trading off entropy. In contrast, LLMs trained without entropy regularization experience rapid entropy collapse, wherein entropy declines to a low value. Correspondingly, the Avg@64 metric rises sharply in the early stages of training but soon plateaus, remaining inferior to that of the model trained with entropy regularization. These results suggest that entropy collapse may lead to performance degradation.

## 5.5 Correlations Between Entropy and Model Performance

The correlations between LLM entropy and performance across benchmarks are task dependent. Specifically, the coding capabilities of LLMs exhibit a strong negative correlation with model entropy during training, whereas performance on tasks involving mathematical reasoning and instruction following shows relatively weak correlations with entropy.

The Pearson correlation coefficients between the entropy of LLMs and their performance across

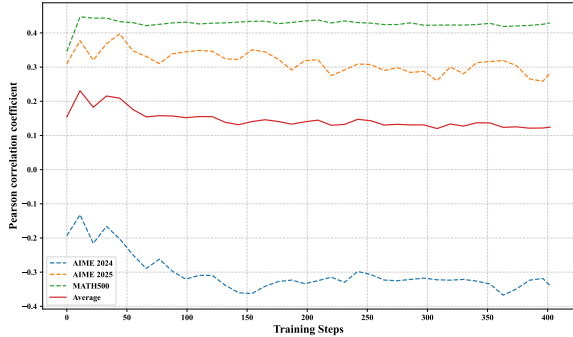


Figure 4: Pearson correlation coefficients between the entropy of LLMs on prompts and their corresponding accuracy across different training steps. “Average” indicates the mean Pearson correlation coefficient computed over AIME 2024, AIME 2025, and MATH500.

	Avg@64	Pass@64
<b>AIME 2024</b>	-0.23107	-0.10477
<b>AIME 2025</b>	-0.29374	0.10454
<b>MATH500</b>	0.11704	0.29805
<b>AMC 2023</b>	-0.18633	0.41696
<b>Minerva</b>	-0.08230	0.38576
<b>LiveCodeBench</b>	<b>-0.79669</b>	<b>-0.71852</b>
<b>IF-Eval</b>	0.67424	-0.61892

Table 1: Pearson correlation coefficients between the entropy of LLMs and their performance across different benchmarks. Coefficients with the largest absolute values are highlighted in bold.

various benchmarks are presented in Table 1. As shown, when LLMs are trained with RLVR using only mathematical data, the Avg@64 and Pass@64 scores on LiveCodeBench exhibit strong negative correlations with model entropy during training, indicating that lower entropy is generally associated with stronger coding capabilities. This relationship is further illustrated in Figure 5, which shows a clear negative correlation between entropy and Avg@64 on LiveCodeBench. By contrast, the correlations between entropy and performance on other benchmarks are relatively weak.

## 5.6 Entropy Collapse and Miscalibration

While RLVR enhances the performance of LLMs, it can lead to miscalibration, causing the models to become increasingly overconfident in their predictions. This miscalibration typically intensifies as entropy collapse becomes more severe. However, incorporating entropy regularization can mitigate this problem.

We further investigate the relationship between

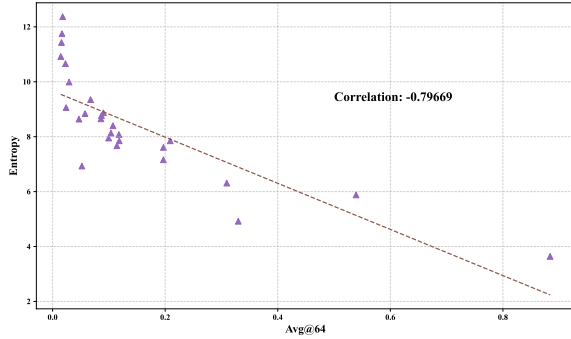


Figure 5: Scatter plot illustrating the relationship between LLM entropy during training and Avg@64 scores on LiveCodeBench. The brown dashed line represents the least-squares regression fit to the data points.

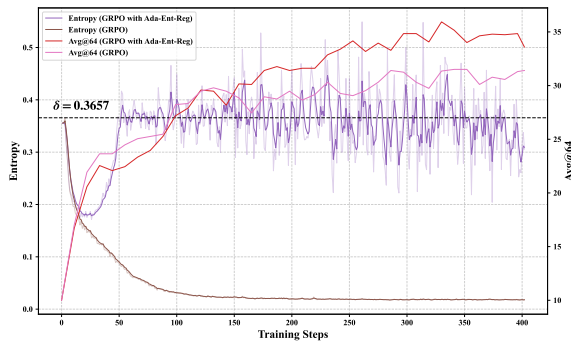


Figure 6: Evolution of the entropy of LLMs during training and their Avg@64 performance on AIME 2024 for models trained with RLVR, with and without adaptive entropy regularization. The predefined entropy threshold  $\delta$  is set to 0.3657, corresponding to the entropy of the LLM on responses to 1,000 randomly sampled prompts from the training dataset prior to training. “Ada-Ent-Reg” denotes adaptive entropy regularization.

entropy and the calibration of LLMs. For a well-calibrated model, correct responses should receive higher probabilities, whereas incorrect ones should be assigned lower probabilities. To assess this, we compute the distributions of average per-token log probabilities for correct and incorrect responses generated by LLMs, as illustrated in Figure 7.

As shown in Figure 7, prior to training, Qwen2.5-Math-7B generally assigns higher probabilities to correct responses than to incorrect ones. However, after GRPO training, the probabilities of both correct and incorrect responses increase, indicating that the model becomes more overconfident. Meanwhile, the probability gap between correct and incorrect responses narrows, suggesting reduced discriminability and poorer calibration, which aligns with the observations of Bereket and Leskovec (2025). Furthermore, when the en-

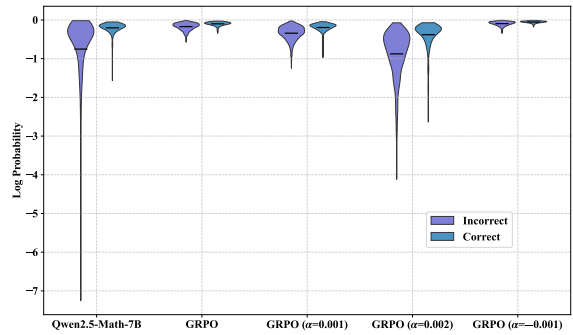


Figure 7: Distribution of log probabilities for correct and incorrect responses across different LLMs. “GRPO” denotes the LLM trained using GRPO, while “GRPO” followed by parentheses indicates LLMs trained with entropy regularization under varying coefficients. In each violin plot, the black line represents the mean.

tropy regularization coefficient is set to a negative value, thereby promoting entropy collapse, both overconfidence and miscalibration become more pronounced. In contrast, employing a positive entropy regularization coefficient mitigates these effects. Considering Figures 7 and 1 jointly, we observe a consistent trend in overconfidence and miscalibration: GRPO ( $\alpha = -0.001$ ) > GRPO > GRPO ( $\alpha = 0.001$ ) > GRPO ( $\alpha = 0.002$ ). A similar ordering is observed for entropy collapse, suggesting a potential correlation between miscalibration and entropy collapse.

## 6 What Factors Govern Entropy Dynamics, Both Theoretically and Empirically?

Previous studies have investigated the factors influencing the entropy of LLMs during training from both theoretical and empirical perspectives. From the theoretical perspective, for example, Liu (2025) and Cui et al. (2025) provided theoretical analyses identifying the factors that govern entropy dynamics during RLVR training. Specifically, they demonstrated that tokens exhibiting strong positive covariance between their probabilities and corresponding advantages primarily drive the substantial entropy reduction observed in RLVR. From the empirical perspective, DAPO (Yu et al., 2025) showed that raising the upper clipping threshold by increasing  $\varepsilon_{\text{high}}$  can alleviate entropy collapse. However, the effect of  $\varepsilon_{\text{low}}$ , which controls the lower clipping threshold, on the entropy and performance of LLMs remains underexplored. Furthermore, empirical evidence from He et al. (2025) suggests

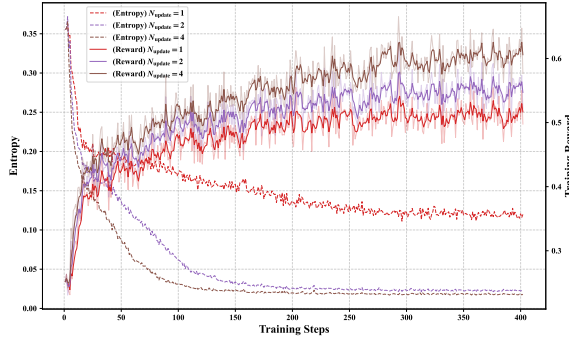


Figure 8: Evolution of the entropy and reward of LLMs during training.

that more off-policy updates exacerbate entropy collapse and degrade LLM performance on test sets. Nevertheless, how off-policy updates influence model performance on the training set remains unclear. To complement these findings, we conduct a series of experiments focusing on three aspects: (1) the effect of off-policy updates on entropy dynamics and model performance on both the training and test sets, (2) the influence of training data diversity on the entropy dynamics of LLMs, and (3) the impact of varying  $\varepsilon_{\text{low}}$  on both model entropy and overall performance.

## 6.1 Off-Policy Updates

More off-policy updates exacerbate entropy collapse, enabling the LLMs to achieve higher rewards on the training set, while their performance improvements on the test set are considerably less pronounced.

In GRPO, a batch of prompts is first sampled and used for rollout, advantage estimation, and the computation of log-probabilities with the LLM employed for rollout. This batch is then divided into several mini-batches, and the model parameters are updated once per mini-batch. Since the parameters change after the first mini-batch update, the data in the remaining mini-batches can be regarded as off-policy data with respect to the updated policy.

To examine the impact of off-policy data on the entropy and reward of LLMs during training, we varied the number of mini-batches per batch, which corresponds to the number of parameter updates per batch and is denoted as  $N_{\text{update}}$ , while keeping the rollout batch size and other hyperparameters fixed. Specifically,  $N_{\text{update}}$  was set to 1, 2, and 4.

Figure 8 presents the evolution of entropy and reward under these configurations. As shown in

the figure, increasing  $N_{\text{update}}$  leads to a more pronounced entropy collapse, consistent with the findings of He et al. (2025), while yielding higher training rewards. Within the reward range of  $[0, 1]$ , increasing  $N_{\text{update}}$  from 1 to 4 raises the training reward by approximately 0.1 (equivalent to a 10% accuracy gain). However, despite this substantial improvement in training reward, Table 3 shows that the corresponding increase in the average Avg@64 score on in-domain test sets remains below 1%. Furthermore, as  $N_{\text{update}}$  increases, the average Pass@64 score declines across both in-domain and out-of-domain benchmarks. These results suggest that more off-policy updates may cause the LLMs to overfit the training set.

## 6.2 Training Data Diversity

Lower data diversity leads to more pronounced entropy collapse during RLVR training. Moreover, training data size is not the only factor determining the performance of LLMs trained with RLVR, as LLMs trained on approximately 600 samples can perform comparably to those trained on about 17k samples.

To examine how training data diversity affects the entropy dynamics of LLMs, we train models on datasets with the same number of samples but different levels of diversity. Specifically, we construct subsets of the original training data using either K-means clustering or random sampling, ensuring that both methods select the same number of samples. Intuitively, subsets derived through K-means clustering are expected to exhibit lower diversity than those obtained via random sampling. Moreover, as the dataset size decreases, the overall data diversity is also expected to decline accordingly.

For subsets constructed using K-means clustering, we apply K-means with the number of clusters  $K = 1,000$ . After clustering, the resulting clusters are sorted in descending order according to their sample counts. Each subset is then formed by selecting samples from the top  $M$  clusters, where  $M$  is set to 281, 112, 49, 21, and 9, corresponding to subsets containing 10,001, 5,031, 2,538, 1,246, and 616 samples, respectively. For subsets constructed via random sampling, we select the same numbers of samples (10,001, 5,031, 2,538, 1,246, and 616) as in the K-means based subsets to ensure a fair comparison. Finally, we train Qwen2.5-Math-7B with RLVR on both the K-means based and ran-

Model	AIME 2024	AIME 2025	MATH500	AMC 2023	Minerva	LiveCodeBench	IF-Eval	Average (ID)	Average (OOD)	Entropy
Qwen2.5-Math-7B	10.00 / 60.00	3.80 / 33.33	43.76 / 95.60	30.04 / 92.50	14.41 / 60.29	3.62 / 30.15	22.67 / 80.46	20.40 / 68.35	13.15 / 55.30	N/A
+ GRPO (Full-data)	28.75 / 63.33	14.69 / 50.00	78.14 / 96.80	64.38 / 97.50	34.64 / 64.34	7.85 / 33.46	30.17 / 72.90	44.12 / 74.39	19.01 / 53.18	0.11838
+ GRPO (10,001 K-means)	31.41 / 63.33	14.22 / 46.67	76.69 / 95.60	64.69 / 95.00	34.38 / 65.81	7.67 / 33.82	29.71 / 73.74	44.28 / 73.28	18.69 / 53.78	0.11419
+ GRPO (10,001 random)	30.00 / 63.33	15.10 / 50.00	77.29 / 96.00	63.48 / 92.50	34.48 / 65.81	8.08 / 35.29	30.56 / 71.46	44.07 / 73.53	19.32 / 53.38	0.11777
+ GRPO (5,031 K-means)	30.16 / 66.67	13.75 / 46.67	74.86 / 95.40	62.85 / 95.00	33.99 / 65.81	8.40 / 34.19	30.90 / 71.58	43.12 / 73.91	19.65 / 52.89	0.10722
+ GRPO (5,031 random)	30.47 / 70.00	14.53 / 50.00	74.80 / 94.80	63.36 / 95.00	33.32 / 64.34	7.95 / 34.93	30.29 / 72.78	43.30 / 74.83	19.12 / 53.85	0.09953
+ GRPO (2,538 K-means)	30.94 / 70.00	13.85 / 46.67	75.29 / 95.40	62.23 / 100.00	34.09 / 63.24	8.77 / 35.66	30.41 / 73.14	43.28 / 75.06	19.59 / 54.40	0.08674
+ GRPO (2,538 random)	30.00 / 70.00	14.32 / 53.33	74.58 / 95.00	63.55 / 95.00	33.67 / 63.24	8.13 / 31.62	29.49 / 72.90	43.22 / 75.31	18.81 / 52.26	0.10369
+ GRPO (1,246 K-means)	30.31 / 70.00	14.01 / 36.67	76.83 / 95.80	63.98 / 95.00	34.71 / 62.50	8.65 / 33.09	30.45 / 71.70	43.97 / 71.99	19.55 / 52.40	0.08588
+ GRPO (1,246 random)	30.47 / 63.33	14.69 / 56.67	75.99 / 95.20	65.27 / 95.00	34.29 / 65.44	8.87 / 34.56	30.47 / 70.50	44.14 / 75.13	19.67 / 52.53	0.09030
+ GRPO (616 K-means)	29.32 / 60.00	17.60 / 46.67	78.57 / 94.80	64.10 / 87.50	36.05 / 59.19	9.06 / 34.93	30.70 / 67.75	45.13 / 69.63	19.88 / 51.34	0.02398
+ GRPO (616 random)	27.55 / 63.33	15.00 / 53.33	68.54 / 89.40	65.27 / 95.00	29.62 / 58.09	9.99 / 36.03	31.23 / 70.26	41.20 / 71.83	20.61 / 53.15	0.02926

Table 2: Performance of Qwen2.5-Math-7B trained with GRPO under varying data scales across multiple benchmarks. ‘‘Entropy’’ denotes the EMA-smoothed entropy at the final training step. Numbers in parentheses indicate the number of training samples, with subscripts ‘‘K-means’’ and ‘‘random’’ referring to datasets selected via K-means clustering and random sampling, respectively. ‘‘Average (ID)’’ and ‘‘Average (OOD)’’ denote the mean performance across in-domain and out-of-domain benchmarks. Results are reported as A / B, corresponding to Avg@64 and Pass@64, evaluated with temperature = 1.0, top- $p$  = 1.0, and a maximum generation length of 4096 tokens.

domly sampled subsets, while keeping all training hyperparameters identical.

Since the entropy of LLMs evolves dynamically during training, we employ an Exponential Moving Average (EMA) to mitigate short-term fluctuations and report the smoothed entropy at the final training step. Formally, at step  $k$ , the EMA-smoothed entropy  $\mathcal{H}_k^{\text{EMA}}$  is defined as:

$$\mathcal{H}_k^{\text{EMA}} = \mathcal{H}_k(\pi_\theta^k) (1 - \varphi) + \varphi \mathcal{H}_{k-1}^{\text{EMA}}, \quad (6)$$

where the smoothing coefficient  $\varphi$  is set to 0.6. The experimental results are summarized in Table 2.

From Table 2, we observe that entropy decreases as the amount of training data decreases. Notably, LLMs trained on subsets constructed via K-means clustering consistently exhibit lower entropy than those trained on randomly sampled subsets, except in the case of models trained on 5,031 samples. These results further demonstrate that training data diversity affects entropy dynamics, as entropy tends to decline when data diversity diminishes. Moreover, Table 2 reveals that, despite a substantial reduction in training data, LLMs trained on considerably smaller subsets can still achieve performance comparable to those trained on the full dataset. This finding indicates that data scale alone does not determine model performance, consistent with prior studies (Li et al., 2025b; Ye et al., 2025; Muennighoff et al., 2025).

### 6.3 Clipping Threshold

A higher upper clipping threshold in GRPO helps alleviate entropy collapse, whereas a lower threshold tends to intensify it. A similar pattern holds for the lower clipping threshold: increasing it mitigates entropy collapse, while decreasing it amplifies the effect. Notably, LLMs can be trained stably even without clipping, achieving performance comparable to that obtained with clipping.

To comprehensively examine how clipping thresholds affect the entropy and performance of LLMs, we trained LLMs with RLVR under various lower and upper clipping thresholds beyond the default setting of  $\varepsilon_{\text{low}} = \varepsilon_{\text{high}} = 0.2$ . Specifically, we conducted the following experiments:

- **Clip-Higher** (Yu et al., 2025) raises the upper clipping bound in the GRPO objective to reduce the proportion of low-probability tokens being clipped. This relaxation allows these tokens to increase their likelihoods more freely, thereby enhancing exploration and mitigating entropy collapse in LLMs. Following Yu et al. (2025), we set  $\varepsilon_{\text{high}} = 0.28$ .
- **Clip-Lower** adopts a similar design to **Clip-Higher** but increases  $\varepsilon_{\text{low}}$ , thereby lowering the clipping lower bound in the GRPO objective. Increasing  $\varepsilon_{\text{low}}$  makes low-probability tokens with negative advantages less susceptible to clipping, allowing their probabilities to decrease more rapidly. Consequently, **Clip-Lower** is expected to intensify entropy col-

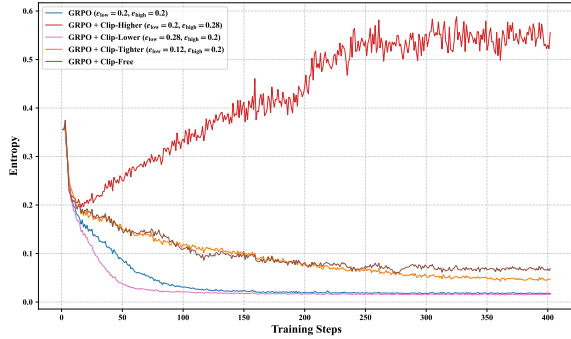


Figure 9: Evolution of the entropy of LLMs during RLVR training with various lower and upper clipping thresholds.

lapse in LLMs. To align the setup with **Clip-Higher**, we set  $\varepsilon_{\text{low}}$  to 0.28.

- **Clip-Tighter**, in contrast to **Clip-Lower**, decreases  $\varepsilon_{\text{low}}$ , thereby raising the clipping lower bound in the GRPO objective. As a result, low-probability tokens with negative advantages become more likely to be clipped, preventing their probabilities from being excessively suppressed. Hence, **Clip-Tighter** is expected to alleviate entropy collapse in LLMs. Specifically, while **Clip-Lower** increases  $\varepsilon_{\text{low}}$  from its default value of 0.2 to 0.28, **Clip-Tighter** decreases  $\varepsilon_{\text{low}}$  by 0.08, resulting in a final value of 0.12.
- **Clip-Free** removes the clipping operation from the GRPO objective. The clipping mechanism, inherited from PPO, serves to penalize updates that deviate substantially from the current policy, thereby stabilizing training. Removing it allows us to examine how clipping influences the entropy dynamics of LLMs and training stability.

The entropy dynamics of LLMs trained with RLVR under various lower and upper clipping thresholds are illustrated in Figure 9. As shown, **Clip-Higher** effectively prevents entropy collapse and even leads to an increase in model entropy during training. In contrast, the other clipping variants (**Clip-Lower**, **Clip-Tighter**, and **Clip-Free**) induce varying degrees of entropy collapse. Among them, **Clip-Lower** results in the most pronounced collapse, whereas **Clip-Tighter** mitigates entropy collapse and maintains higher entropy compared to the default clipping configuration ( $\varepsilon_{\text{low}} = \varepsilon_{\text{high}} = 0.2$ ).

These observations align with theoretical expectations. **Clip-Higher** expands the upper clip-

ping bound, allowing low-probability tokens with positive advantages to avoid being clipped. Consequently, these tokens can increase their probabilities during training, mitigating the over-concentration of the probability distribution across the vocabulary and preventing entropy collapse. Conversely, **Clip-Lower** decreases the lower clipping bound, enabling low-probability tokens with negative advantages to be excluded from clipping. This allows their probabilities to decrease further, thereby exacerbating the over-concentration of the distribution and intensifying entropy collapse. In comparison, **Clip-Tighter** raises the lower clipping bound, making low-probability tokens with negative advantages more likely to be clipped. As a result, their probabilities are preserved during training, which helps alleviate entropy collapse.

Surprisingly, Figure 9 shows that **Clip-Free** attains the highest entropy among all clipping variants (including the default clipping configuration), except for **Clip-Higher**. Moreover, as presented in Table 3, on in-domain test sets, **Clip-Free** yields the second-highest average Avg@64 and Pass@64 scores among all clipping variants. On out-of-domain test sets, **Clip-Free** similarly achieves the second-highest Avg@64 and the highest average Pass@64. These results suggest that the clipping operation in the GRPO objective, which is designed to prevent excessively large updates during training, can be removed without compromising the stability of RLVR training.

## 7 How Can Entropy Be Effectively Regulated to Improve the Performance of LLMs?

To effectively regulate entropy, we first examine which types of tokens that drive entropy changes during training. Liu (2025) and Cui et al. (2025) mathematically proved that the entropy change of an LLM between two consecutive training steps can be approximated by the product of the learning rate and the covariance between  $\log \pi_{\theta}^k(\mathbf{y}_t | \mathbf{x}, \mathbf{y}_{<t})$  and  $\pi_{\theta}^k(\mathbf{y}_t | \mathbf{x}, \mathbf{y}_{<t}) \hat{A}_t$ . This implies that tokens with both high probabilities and high advantages, or low probabilities and low advantages, primarily contribute to the entropy collapse. However, we posit that tokens with low probabilities and low advantages occur infrequently, as high-probability tokens are more likely to be sampled during decoding and thus dominate model-generated responses. Based on this intuition, we hypothesize that the

Model	AIME 2024	AIME 2025	MATH500	AMC 2023	Minerva	LiveCodeBench	IF-Eval	Average (ID)	Average (OOD)	Entropy
Qwen2.5-Math-7B	10.00 / 60.00	3.80 / 33.33	43.76 / 95.60	30.04 / 92.50	14.41 / 60.29	3.62 / 30.15	22.67 / 80.46	20.40 / 68.35	13.15 / 55.30	N/A
+ GRPO ( $N_{\text{update}} = 1$ )	28.75 / 63.33	14.69 / 50.00	78.14 / 96.80	64.38 / 97.50	34.64 / 64.34	7.85 / 33.46	30.17 / 72.90	44.12 / 74.39	19.01 / 53.18	0.11838
+ GRPO ( $N_{\text{update}} = 2$ )	29.58 / 70.00	16.98 / 46.67	76.56 / 94.40	67.42 / 92.50	33.28 / 62.50	10.66 / 34.56	28.72 / 71.10	44.76 / 73.21	19.69 / 52.83	0.02286
+ GRPO ( $N_{\text{update}} = 4$ )	31.41 / 63.33	14.90 / 56.67	72.09 / 90.80	75.43 / 90.00	31.14 / 55.51	12.37 / 34.56	29.83 / 70.38	44.99 / 71.26	21.10 / 52.47	0.01789
+ Clip-Higher	33.33 / 60.00	15.94 / 53.33	72.35 / 94.20	67.62 / 97.50	30.57 / 63.97	5.88 / 32.35	31.35 / 66.19	43.96 / 73.80	18.62 / 49.27	0.53910
+ Clip-Lower	27.76 / 56.67	15.31 / 50.00	71.61 / 89.20	74.73 / 87.50	30.07 / 55.51	11.43 / 31.99	28.10 / 66.91	43.90 / 67.78	19.76 / 49.45	0.01577
+ Clip-Tighter	32.19 / 63.33	16.09 / 43.33	67.59 / 90.40	69.18 / 95.00	26.03 / 54.78	8.64 / 34.56	29.96 / 69.06	42.22 / 69.37	19.30 / 51.81	0.04681
+ Clip-Free	34.38 / 66.67	17.19 / 43.33	73.02 / 92.40	69.14 / 97.50	31.01 / 59.93	9.35 / 34.93	30.53 / 70.50	44.95 / 71.97	19.94 / 52.72	0.06745
+ Ada-Ent-Reg ( $\delta = 0.2$ )	32.92 / 66.67	16.30 / 50.00	69.05 / 90.40	69.34 / 92.50	27.63 / 61.03	7.16 / 33.09	31.26 / 68.94	43.05 / 72.12	19.21 / 51.02	0.19692
+ Ada-Ent-Reg ( $\delta = 0.3657$ )	33.96 / 66.67	18.65 / 50.00	73.98 / 92.80	68.52 / 97.50	31.66 / 61.76	6.31 / 32.35	29.66 / 69.78	45.35 / 73.75	17.98 / 51.07	0.30941
+ Clip-Cov	31.98 / 70.00	18.18 / 53.33	74.27 / 95.80	68.13 / 97.50	32.23 / 62.50	7.85 / 34.56	31.05 / 69.06	44.96 / 75.83	19.45 / 51.81	0.20899
+ KL-Cov	33.96 / 66.67	16.20 / 53.33	70.10 / 93.60	68.79 / 97.50	28.63 / 61.03	7.61 / 34.93	30.82 / 68.35	43.54 / 74.43	19.21 / 51.64	0.19695
+ Entropy-Adv	31.09 / 66.67	15.52 / 46.67	76.65 / 93.60	70.63 / 87.50	33.80 / 60.29	11.75 / 31.25	29.21 / 70.14	45.54 / 70.95	20.48 / 50.70	0.01669
+ Adv $\leq 0$	29.79 / 63.33	11.04 / 46.67	76.55 / 96.00	63.40 / 97.50	32.73 / 63.97	3.64 / 26.47	33.70 / 62.11	42.70 / 73.49	18.67 / 44.29	0.88384
+ Adv $\geq 0$	27.55 / 53.33	13.23 / 43.33	72.20 / 91.00	64.49 / 92.50	34.05 / 58.09	10.92 / 33.46	28.17 / 71.58	42.30 / 67.65	19.55 / 52.52	0.01460
+ Rand-Pos-Clip	34.27 / 66.67	16.93 / 46.67	73.21 / 93.80	68.13 / 97.50	31.86 / 61.03	8.84 / 34.19	30.74 / 69.54	44.88 / 73.13	19.79 / 51.87	0.05763
+ Prog-Adv-Reweight-1	31.72 / 56.67	15.21 / 46.67	78.79 / 96.00	64.84 / 95.00	33.67 / 65.81	4.92 / 31.99	33.07 / 60.91	44.85 / 72.03	19.00 / 46.45	0.32983
+ Prog-Adv-Reweight-2	32.34 / 66.67	17.45 / 43.33	75.75 / 95.40	66.17 / 95.00	33.51 / 60.29	6.93 / 33.46	31.63 / 66.43	45.05 / 72.14	19.28 / 49.94	0.05203

Table 3: Performance of Qwen2.5-Math-7B trained with GRPO and its entropy-regularized variants. “Ada-Ent-Reg” denotes Adaptive Entropy Regularization. “Average (ID)” and “Average (OOD)” indicate the mean performance across in-domain and out-of-domain benchmarks, respectively. Results are presented as A / B, representing Avg@64 and Pass@64, evaluated with temperature = 1.0, top- $p$  = 1.0, and a maximum generation length of 4096 tokens.

entropy collapse of LLMs mainly stems from tokens with high advantages, and we further provide a theoretical derivation to support this hypothesis.

Let  $z_v$  denote the logit of token  $v$  produced by the LLM. When token  $v$  is not sampled in the generation of token  $\mathbf{y}_t$ , the gradient of the GRPO objective with respect to  $z_v$  can be approximated as:

$$\begin{aligned} \frac{\partial \mathcal{J}(\theta)}{\partial z_v} &= -\mathbb{E}_{\mathbf{y}_t \sim \pi_\theta(\cdot | \mathbf{x}, \mathbf{y}_{< t})} \pi_\theta(v | \mathbf{x}, \mathbf{y}_{< t}) \hat{A}_t \\ &\approx -\pi_\theta(v | \mathbf{x}, \mathbf{y}_{< t}) \hat{A}_t \end{aligned} \quad (7)$$

Similarly, when token  $v$  is sampled in generating token  $\mathbf{y}_t$ , the gradient of the GRPO objective with respect to  $z_v$  can be approximated as:

$$\begin{aligned} \frac{\partial \mathcal{J}(\theta)}{\partial z_v} &= \mathbb{E}_{\mathbf{y}_t \sim \pi_\theta(\cdot | \mathbf{x}, \mathbf{y}_{< t})} (1 - \pi_\theta(v | \mathbf{x}, \mathbf{y}_{< t})) \hat{A}_t \\ &\approx (1 - \pi_\theta(v | \mathbf{x}, \mathbf{y}_{< t})) \hat{A}_t \end{aligned} \quad (8)$$

The detailed derivations of the above approximations are provided in Appendix C. These approximations theoretically indicate that tokens with positive advantages drive the entropy collapse of LLMs during training. Specifically, since RLR performs gradient ascent to maximize the optimization objective, a positive advantage implies that the update increases the probabilities of sampled tokens while decreasing those of unsampled ones. Given that high-probability tokens are more likely to be sampled, this process concentrates the probability mass and thus exacerbates entropy collapse. Conversely, when the advantages are negative, the update reduces the probabilities of sampled tokens and in-

creases those of unsampled tokens. In this case, because high-probability tokens are again more likely to be sampled, the update counteracts the tendency toward over-concentration of probabilities, thereby alleviating entropy collapse.

To empirically validate this hypothesis, we conducted two comparative experiments: training LLMs solely on tokens with advantages  $\geq 0$  and solely on tokens with advantages  $\leq 0$ , and compared these settings with the following baselines:

- **Adaptive Entropy Regularization** dynamically adjusts the entropy regularization coefficient to keep model entropy above a predefined threshold  $\delta$ . We consider two settings for  $\delta$ : (1)  $\delta = 0.2$ , following He et al. (2025), and (2)  $\delta$  set to the entropy of the LLM on responses to 1,000 randomly sampled training prompts before training, which equals 0.3657.
- **Clip-Cov** (Cui et al., 2025) mitigates entropy collapse by zeroing the gradients of a small subset of tokens with high covariance between log probabilities and advantages.
- **KL-Cov** (Cui et al., 2025) adopts a similar approach to Clip-Cov but applies a KL penalty to high-covariance tokens.
- **Entropy-Adv** (Cheng et al., 2025) augments the original advantage with an entropy term to encourage exploratory reasoning tokens and enhance LLM performance.

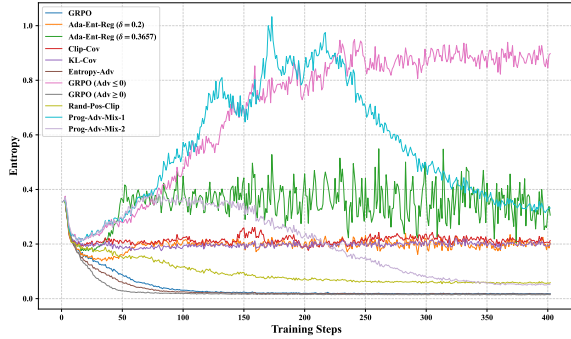


Figure 10: Evolution of the entropy of LLMs during RLVR training under different methods. “Ada-Ent-Reg” denotes Adaptive Entropy Regularization.

- **Rand-Pos-Clip** serves as a counterpart to **Clip-Cov**. Unlike **Clip-Cov**, which sets the gradients of a small subset of tokens exhibiting high covariance between log probabilities and advantages to zero, **Rand-Pos-Clip** randomly zeroes the gradients of a subset of tokens with positive advantages. To ensure a fair comparison between the two methods, we maintain the same proportion of tokens whose gradients are set to zero in both **Rand-Pos-Clip** and **Clip-Cov**.

As shown in Section 5, increasing the number of parameter updates per batch ( $N_{\text{update}}$ ) intensifies entropy collapse. Accordingly, we primarily conduct experiments under the setting where  $N_{\text{update}}$  is fixed at 4 to evaluate the effectiveness of different approaches in controlling the entropy of LLMs.

Figure 10 illustrates the evolution of entropy across different methods. As shown, **Clip-Cov**, **KL-Cov**, **Adaptive Entropy Regularization**, and **Rand-Pos-Clip** effectively alleviate entropy collapse, whereas **Ent-Adv** intensifies it. Furthermore, we observe that training LLMs exclusively on tokens with advantages  $\geq 0$  leads to the most severe entropy collapse, while training on tokens with advantages  $\leq 0$  drives entropy to a high level. These findings empirically support our hypothesis that entropy collapse primarily stems from tokens with high advantages, implying that adjusting the relative loss weights of tokens with advantages  $\geq 0$  and  $\leq 0$  can regulate model entropy.

Building on this insight, we propose **Progressive Advantage Reweighting (Prog-Adv-Reweighting)**, which controls entropy by dynamically adjusting the loss weights assigned to tokens with non-negative advantages. Specifically, we introduce a hyperparameter  $\lambda$  that determines the loss weights

of tokens with advantages  $\geq 0$ . We propose two variants of **Prog-Adv-Reweighting**, distinguished by the way the  $\lambda$  changes during training:

- **Prog-Adv-Reweighting-1** partitions the RLVR training process into two stages, each comprising an equal number of training steps. In the first stage,  $\lambda$  is fixed at 0, meaning the model is trained solely on tokens with non-positive advantages. In the second stage,  $\lambda$  increases linearly from 0 to 1, progressively enhancing the contributions of positive-advantage tokens as training advances.
- **Prog-Adv-Reweighting-2** increases  $\lambda$  linearly across epochs, from 0 in the first epoch to 1 in the final epoch. If the total number of epochs is  $E$  and the current epoch is  $e$ , then  $\lambda$  is defined as  $\lambda = (e - 1)/(E - 1)$ .

As shown in Figure 10, both **Prog-Adv-Reweighting-1** and **Prog-Adv-Reweighting-2** induce an initial rise in entropy followed by a gradual decline, indicating that entropy decreases as the loss weights of tokens with positive advantages increase. This observation confirms that adjusting the relative loss weights of tokens with positive and negative advantages effectively regulates entropy.

Table 3 summarizes the performance of LLMs trained with RLVR under various entropy regularization approaches across multiple benchmarks. As shown in Table 3, although training exclusively on tokens with advantages  $\leq 0$  effectively mitigates entropy collapse, it results in lower average Avg@64 scores on both in-domain and out-of-domain benchmarks, as well as reduced average Pass@64 scores on out-of-domain benchmarks. In contrast, by dynamically adjusting the loss weights of tokens with non-negative advantages during training, both **Prog-Adv-Reweighting-1** and **Prog-Adv-Reweighting-2** further improve LLM performance beyond the  $\text{Adv} \leq 0$  setting and achieve results comparable to other entropy regularization methods. These findings demonstrate that **Progressive Advantage Reweighting** effectively mitigates entropy collapse while maintaining competitive performance. Moreover, despite its simplicity, **Rand-Pos-Clip**, which randomly sets the gradients of a small subset of tokens with positive advantages to zero, achieves an average Avg@64 score comparable to that of **Clip-Cov** on both in-domain and out-of-domain benchmarks, and a comparable average Pass@64 score on out-of-domain benchmarks.

## 8 Conclusion

In this paper, we comprehensively investigate the entropy dynamics of LLMs trained with RLVR. Through extensive empirical analyses, we examine how the entropy of LLMs correlates with response diversity, model calibration, and performance across multiple benchmarks. Furthermore, we identify three key factors that critically influence the entropy dynamics of LLMs: the number of off-policy updates, training data diversity, and the clipping threshold. Our theoretical and empirical analyses further reveal that entropy collapse primarily arises from tokens with positive advantages, and that entropy can be effectively regulated by adjusting the relative loss weights assigned to tokens with positive and negative advantages. Building on these insights, we propose **Progressive Advantage Reweighting (Prog-Adv-Reweight)**, a simple yet effective approach that dynamically adjusts the loss weights of tokens with positive advantages during training, thereby mitigating entropy collapse while maintaining competitive performance compared with other entropy regularization methods across benchmarks.

## Limitations

Due to computational constraints, our experiments were conducted solely on Qwen2.5-Math-7B. As LLMs vary in their pre-training data, training strategies, and architectures, some of our findings may not generalize directly to other models. Nevertheless, we hope that our analysis of entropy dynamics in RLVR training provides valuable empirical insights for the research community and motivates the development of more effective entropy regularization methods in future work.

## References

Michael Bereket and Jure Leskovec. 2025. [Uncalibrated reasoning: GRPO induces overconfidence for stochastic outcomes](#). *CoRR*, abs/2508.11800.

Zhipeng Chen, Xiaobo Qin, Youbin Wu, Yue Ling, Qinghao Ye, Wayne Xin Zhao, and Guang Shi. 2025. [Pass@k training for adaptively balancing exploration and exploitation of large reasoning models](#). *CoRR*, abs/2508.10751.

Daixuan Cheng, Shaohan Huang, Xuekai Zhu, Bo Dai, Wayne Xin Zhao, Zhenliang Zhang, and Furu Wei. 2025. [Reasoning with exploration: An entropy perspective](#). *CoRR*, abs/2506.14758.

Ganqu Cui, Yuchen Zhang, Jiacheng Chen, Lifan Yuan, Zhi Wang, Yuxin Zuo, Haozhan Li, Yuchen Fan, Huayu Chen, Weize Chen, Zhiyuan Liu, Hao Peng, Lei Bai, Wanli Ouyang, Yu Cheng, Bowen Zhou, and Ning Ding. 2025. [The entropy mechanism of reinforcement learning for reasoning language models](#). *CoRR*, abs/2505.22617.

DeepSeek-AI, Daya Guo, Dejian Yang, Haowei Zhang, Junxiao Song, Ruoyu Zhang, Runxin Xu, Qihao Zhu, Shirong Ma, Peiyi Wang, Xiao Bi, Xiaokang Zhang, Xingkai Yu, Yu Wu, Z. F. Wu, Zhibin Gou, Zhi-hong Shao, Zhuoshu Li, Ziyi Gao, and 81 others. 2025. [Deepseek-r1: Incentivizing reasoning capability in llms via reinforcement learning](#). *CoRR*, abs/2501.12948.

Jia Deng, Jie Chen, Zhipeng Chen, Wayne Xin Zhao, and Ji-Rong Wen. 2025. [Decomposing the entropy-performance exchange: The missing keys to unlocking effective reinforcement learning](#). *CoRR*, abs/2508.02260.

Jujie He, Jiacai Liu, Chris Yuhao Liu, Rui Yan, Chaojie Wang, Peng Cheng, Xiaoyu Zhang, Fuxiang Zhang, Jiacheng Xu, Wei Shen, Siyuan Li, Liang Zeng, Tianwen Wei, Cheng Cheng, Bo An, Yang Liu, and Yahui Zhou. 2025. [Skywork open reasoner 1 technical report](#). *CoRR*, abs/2505.22312.

Dan Hendrycks, Collin Burns, Saurav Kadavath, Akul Arora, Steven Basart, Eric Tang, Dawn Song, and Jacob Steinhardt. 2021. [Measuring mathematical problem solving with the MATH dataset](#). In *Proceedings of the Neural Information Processing Systems Track on Datasets and Benchmarks 1, NeurIPS Datasets and Benchmarks 2021, December 2021, virtual*.

Aaron Jaech, Adam Kalai, Adam Lerer, Adam Richardson, Ahmed El-Kishky, Aiden Low, Alec Hel-lyar, Aleksander Madry, Alex Beutel, Alex Carney, Alex Iftimie, Alex Karpenko, Alex Tachard Passos, Alexander Neitz, Alexander Prokofiev, Alexander Wei, Allison Tam, Ally Bennett, Ananya Kumar, and 80 others. 2024. [Openai o1 system card](#). *CoRR*, abs/2412.16720.

Naman Jain, King Han, Alex Gu, Wen-Ding Li, Fanjia Yan, Tianjun Zhang, Sida Wang, Armando Solar-Lezama, Koushik Sen, and Ion Stoica. 2025. [Live-codebench: Holistic and contamination free evaluation of large language models for code](#). In *The Thirteenth International Conference on Learning Representations, ICLR 2025, Singapore, April 24-28, 2025*. OpenReview.net.

Aitor Lewkowycz, Anders Andreassen, David Dohan, Ethan Dyer, Henryk Michalewski, Vinay V. Ramaresh, Ambrose Slone, Cem Anil, Imanol Schlag, Theo Gutman-Solo, Yuhuai Wu, Behnam Neyshabur, Guy Gur-Ari, and Vedant Misra. 2022. [Solving quantitative reasoning problems with language models](#). In *Advances in Neural Information Processing Systems 35: Annual Conference on Neural Information Processing Systems 2022, NeurIPS 2022, New Orleans, LA, USA, November 28 - December 9, 2022*.

Jiwei Li, Michel Galley, Chris Brockett, Jianfeng Gao, and Bill Dolan. 2016. **A diversity-promoting objective function for neural conversation models**. In *NAACL HLT 2016, The 2016 Conference of the North American Chapter of the Association for Computational Linguistics: Human Language Technologies, San Diego California, USA, June 12-17, 2016*, pages 110–119. The Association for Computational Linguistics.

Qingbin Li, Rongkun Xue, Jie Wang, Ming Zhou, Zhi Li, Xiaofeng Ji, Yongqi Wang, Miao Liu, Zheming Yang, Minghui Qiu, and Jing Yang. 2025a. **CURE: critical-token-guided re-concatenation for entropy-collapse prevention**. *CoRR*, abs/2508.11016.

Xuefeng Li, Haoyang Zou, and Pengfei Liu. 2025b. **LIMR: less is more for RL scaling**. *CoRR*, abs/2502.11886.

Jiacai Liu. 2025. **How does rl policy entropy converge during iteration?** <https://zhuanlan.zhihu.com/p/28476703733>.

Zheng Liu, Mengjie Liu, Siwei Wen, Mengzhang Cai, Bin Cui, Conghui He, and Wentao Zhang. 2025a. **From uniform to heterogeneous: Tailoring policy optimization to every token’s nature**. *Preprint*, arXiv:2509.16591.

Zichen Liu, Changyu Chen, Wenjun Li, Penghui Qi, Tianyu Pang, Chao Du, Wee Sun Lee, and Min Lin. 2025b. **Understanding r1-zero-like training: A critical perspective**. *CoRR*, abs/2503.20783.

Michael Luo, Sijun Tan, Roy Huang, Ameen Patel, Alpay Ariyak, Qingyang Wu, Xiaoxiang Shi, Rachel Xin, Colin Cai, Maurice Weber, Ce Zhang, Li Erran Li, Raluca Ada Popa, and Ion Stoica. 2025. **Deepcoder: A fully open-source 14b coder at o3-mini level**. Notion Blog.

MAA. 2023. American Mathematics Competitions - AMC 2023.

MAA. 2024. American Invitational Mathematics Examination - AIME 2024.

MAA. 2025. American Invitational Mathematics Examination - AIME 2025.

Niklas Muennighoff, Zitong Yang, Weijia Shi, Xiang Lisa Li, Li Fei-Fei, Hannaneh Hajishirzi, Luke Zettlemoyer, Percy Liang, Emmanuel J. Candès, and Tatsunori Hashimoto. 2025. **s1: Simple test-time scaling**. *CoRR*, abs/2501.19393.

John Schulman, Filip Wolski, Prafulla Dhariwal, Alec Radford, and Oleg Klimov. 2017. **Proximal policy optimization algorithms**. *CoRR*, abs/1707.06347.

Zhihong Shao, Peiyi Wang, Qihao Zhu, Runxin Xu, Junxiao Song, Mingchuan Zhang, Y. K. Li, Y. Wu, and Daya Guo. 2024. **Deepseekmath: Pushing the limits of mathematical reasoning in open language models**. *CoRR*, abs/2402.03300.

Han Shen. 2025. **On entropy control in llm-rl algorithms**. *Preprint*, arXiv:2509.03493.

Guangming Sheng, Chi Zhang, Zilingfeng Ye, Xibin Wu, Wang Zhang, Ru Zhang, Yanghua Peng, Haibin Lin, and Chuan Wu. 2025. **Hybridflow: A flexible and efficient RLHF framework**. In *Proceedings of the Twentieth European Conference on Computer Systems, EuroSys 2025, Rotterdam, The Netherlands, 30 March 2025 - 3 April 2025*, pages 1279–1297. ACM.

Zhenpeng Su, Leiyu Pan, Minxuan Lv, Yuntao Li, Wengping Hu, Fuzheng Zhang, Kun Gai, and Guorui Zhou. 2025. **Ce-gppo: Coordinating entropy via gradient-preserving clipping policy optimization in reinforcement learning**. *Preprint*, arXiv:2509.20712.

Jiawei Wang, Jiacai Liu, Yuqian Fu, Yingru Li, Xintao Wang, Yuan Lin, Yu Yue, Lin Zhang, Yang Wang, and Ke Wang. 2025a. **Harnessing uncertainty: Entropy-modulated policy gradients for long-horizon llm agents**. *Preprint*, arXiv:2509.09265.

Shenzhi Wang, Le Yu, Chang Gao, Chujie Zheng, Shixuan Liu, Rui Lu, Kai Dang, Xionghui Chen, Jianxin Yang, Zhenru Zhang, Yuqiong Liu, An Yang, Andrew Zhao, Yang Yue, Shiji Song, Bowen Yu, Gao Huang, and Junyang Lin. 2025b. **Beyond the 80/20 rule: High-entropy minority tokens drive effective reinforcement learning for LLM reasoning**. *CoRR*, abs/2506.01939.

Mingqi Wu, Zhihao Zhang, Qiaole Dong, Zhiheng Xi, Jun Zhao, Senjie Jin, Xiaoran Fan, Yuhao Zhou, Yanwei Fu, Qin Liu, Songyang Zhang, and Qi Zhang. 2025. **Reasoning or memorization? unreliable results of reinforcement learning due to data contamination**. *CoRR*, abs/2507.10532.

An Yang, Beichen Zhang, Binyuan Hui, Bofei Gao, Bowen Yu, Chengpeng Li, Dayiheng Liu, Jianhong Tu, Jingren Zhou, Junyang Lin, Keming Lu, Mingfeng Xue, Runji Lin, Tianyu Liu, Xingzhang Ren, and Zhenru Zhang. 2024. **Qwen2.5-math technical report: Toward mathematical expert model via self-improvement**. *CoRR*, abs/2409.12122.

Yixin Ye, Zhen Huang, Yang Xiao, Ethan Chern, Shijie Xia, and Pengfei Liu. 2025. **LIMO: less is more for reasoning**. *CoRR*, abs/2502.03387.

Qiying Yu, Zheng Zhang, Ruofei Zhu, Yufeng Yuan, Xiaochen Zuo, Yu Yue, Tiantian Fan, Gaohong Liu, Lingjun Liu, Xin Liu, Haibin Lin, Zhiqi Lin, Bole Ma, Guangming Sheng, Yuxuan Tong, Chi Zhang, Mofan Zhang, Wang Zhang, Hang Zhu, and 16 others. 2025. **DAPO: an open-source LLM reinforcement learning system at scale**. *CoRR*, abs/2503.14476.

Jeffrey Zhou, Tianjian Lu, Swaroop Mishra, Siddhartha Brahma, Sujoy Basu, Yi Luan, Denny Zhou, and Le Hou. 2023. **Instruction-following evaluation for large language models**. *CoRR*, abs/2311.07911.

Xinyu Zhu, Mengzhou Xia, Zhepei Wei, Wei-Lin Chen, Danqi Chen, and Yu Meng. 2025. [The surprising effectiveness of negative reinforcement in LLM reasoning](#). *CoRR*, abs/2506.01347.

Yaoming Zhu, Sidi Lu, Lei Zheng, Jiaxian Guo, Weinan Zhang, Jun Wang, and Yong Yu. 2018. [Texxygen: A benchmarking platform for text generation models](#). In *The 41st International ACM SIGIR Conference on Research & Development in Information Retrieval, SIGIR 2018, Ann Arbor, MI, USA, July 08-12, 2018*, pages 1097–1100. ACM.

Brian D. Ziebart. 2010. [Modeling Purposeful Adaptive Behavior with the Principle of Maximum Causal Entropy](#). Ph.D. thesis, Carnegie Mellon University, USA.

Brian D. Ziebart, Andrew L. Maas, J. Andrew Bagnell, and Anind K. Dey. 2008. [Maximum entropy inverse reinforcement learning](#). In *Proceedings of the Twenty-Third AAAI Conference on Artificial Intelligence, AAAI 2008, Chicago, Illinois, USA, July 13-17, 2008*, pages 1433–1438. AAAI Press.

## A Experimental Setup

The diversity of responses generated by LLMs is evaluated using the N-gram Diversity (Li et al., 2016) and SelfBLEU (Zhu et al., 2018) metrics. Specifically, the N-gram Diversity metric quantifies the proportion of unique n-grams relative to the total number of n-grams in the generated responses. Let  $U_i$  denote the number of unique n-grams and  $C_i$  the total number of n-grams of order  $i$ . The metric is formally defined as

$$\text{N-gram Diversity} = \prod_{i=1}^N \frac{U_i}{C_i}. \quad (9)$$

In our experiments, we set  $N = 5$  when applying the N-gram Diversity metric to assess response diversity.

The SelfBLEU metric measures diversity from a complementary perspective. For each response, the BLEU score is computed by treating it as the hypothesis and all other responses as references. The resulting BLEU scores, averaged over 1- to 4-gram, are then averaged across all responses to obtain the final SelfBLEU score.

## B How Does the Entropy of LLMs Trained with RLVR Correlate with Their Performance?

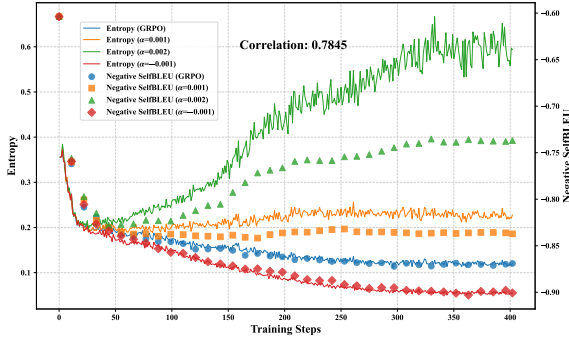


Figure 11: Evolution of entropy (solid lines) and negative SelfBLEU (markers) over training steps under different entropy regularization settings.

## C How Can Entropy Be Effectively Regulated to Improve the Performance of LLMs?

To clearly illustrate the derivation of the gradient of the GRPO optimization objective with respect to the logit  $z_v$  of token  $v$ , we simplify the original

GRPO objective by assuming that the LLM performs on-policy updates. Under this assumption, the importance ratio and the clipping term in the original objective can be omitted. Consequently, the GRPO optimization objective can be simplified as follows:

$$\mathcal{J}(\theta) = \mathbb{E}_{\mathbf{y}_t \sim \pi_\theta(\cdot | \mathbf{x}, \mathbf{y}_{<t})} \hat{A}_t \quad (10)$$

The gradient of the simplified GRPO objective with respect to the logit  $z_v$  of token  $v$  is given by:

$$\begin{aligned} \frac{\partial \mathcal{J}(\theta)}{\partial z_v} &= \frac{\partial \mathbb{E}_{\mathbf{y}_t \sim \pi_\theta(\cdot | \mathbf{x}, \mathbf{y}_{<t})} \hat{A}_t}{\partial z_v} \\ &= \frac{\partial \sum_{\mathbf{y}_t} \pi_\theta(\mathbf{y}_t | \mathbf{x}, \mathbf{y}_{<t}) \hat{A}_t}{\partial z_v} \\ &= \frac{\sum_{\mathbf{y}_t} \partial \pi_\theta(\mathbf{y}_t | \mathbf{x}, \mathbf{y}_{<t}) \hat{A}_t}{\partial z_v} \\ &= \frac{\sum_{\mathbf{y}_t} \pi_\theta(\mathbf{y}_t | \mathbf{x}, \mathbf{y}_{<t}) \partial \log \pi_\theta(\mathbf{y}_t | \mathbf{x}, \mathbf{y}_{<t}) \hat{A}_t}{\partial z_v} \\ &= \frac{\mathbb{E}_{\mathbf{y}_t \sim \pi_\theta(\cdot | \mathbf{x}, \mathbf{y}_{<t})} \partial \log \pi_\theta(\mathbf{y}_t | \mathbf{x}, \mathbf{y}_{<t}) \hat{A}_t}{\partial z_v} \\ &= \frac{\mathbb{E}_{\mathbf{y}_t \sim \pi_\theta(\cdot | \mathbf{x}, \mathbf{y}_{<t})} \partial \pi_\theta(\mathbf{y}_t | \mathbf{x}, \mathbf{y}_{<t}) \hat{A}_t}{\pi_\theta(\mathbf{y}_t | \mathbf{x}, \mathbf{y}_{<t}) \partial z_v} \end{aligned} \quad (11)$$

When token  $v$  is **not** sampled during the generation of  $\mathbf{y}_t$ , the gradient of  $\pi_\theta(\mathbf{y}_t | \mathbf{x}, \mathbf{y}_{<t})$  with respect to  $z_v$  is:

$$\begin{aligned} \partial \pi_\theta(\mathbf{y}_t | \mathbf{x}, \mathbf{y}_{<t}) &= \frac{\partial \frac{\exp(z_{\mathbf{y}_t})}{\sum_{v' \in \mathcal{V}} \exp(z_{v'})}}{\partial z_v} \\ &= \frac{-\exp(z_{\mathbf{y}_t}) \exp(z_v)}{(\sum_{v' \in \mathcal{V}} \exp(z_{v'}))^2} \\ &= -\pi_\theta(\mathbf{y}_t | \mathbf{x}, \mathbf{y}_{<t}) \pi_\theta(v | \mathbf{x}, \mathbf{y}_{<t}) \end{aligned} \quad (12)$$

Conversely, when token  $v$  is sampled during the generation of  $\mathbf{y}_t$ , the gradient becomes:

$$\begin{aligned} \partial \pi_\theta(\mathbf{y}_t | \mathbf{x}, \mathbf{y}_{<t}) &= \frac{\partial \frac{\exp(z_{\mathbf{y}_t})}{\sum_{v' \in \mathcal{V}} \exp(z_{v'})}}{\partial z_v} \\ &= \frac{\exp(z_{\mathbf{y}_t}) \sum_{v' \in \mathcal{V}} \exp(z_{v'}) - \exp(z_{\mathbf{y}_t})^2}{(\sum_{v' \in \mathcal{V}} \exp(z_{v'}))^2} \\ &= \frac{\exp(z_{\mathbf{y}_t})}{(\sum_{v' \in \mathcal{V}} \exp(z_{v'}))} - \frac{\exp(z_{\mathbf{y}_t})^2}{(\sum_{v' \in \mathcal{V}} \exp(z_{v'}))^2} \\ &= \pi_\theta(\mathbf{y}_t | \mathbf{x}, \mathbf{y}_{<t}) - \pi_\theta(\mathbf{y}_t | \mathbf{x}, \mathbf{y}_{<t})^2 \\ &= \pi_\theta(\mathbf{y}_t | \mathbf{x}, \mathbf{y}_{<t}) (1 - \pi_\theta(\mathbf{y}_t | \mathbf{x}, \mathbf{y}_{<t})) \end{aligned} \quad (13)$$

By substituting Eq. (12) into Eq. (11), we obtain the gradient of the simplified GRPO objective with respect to  $z_v$  when token  $v$  is **not** sampled:

$$\begin{aligned} \frac{\partial \mathcal{J}(\theta)}{\partial z_v} &= \frac{\mathbb{E}_{\mathbf{y}_t \sim \pi_\theta(\cdot | \mathbf{x}, \mathbf{y}_{<t})} \partial \pi_\theta(\mathbf{y}_t | \mathbf{x}, \mathbf{y}_{<t}) \hat{A}_t}{\pi_\theta(\mathbf{y}_t | \mathbf{x}, \mathbf{y}_{<t}) \partial z_v} \\ &= -\mathbb{E}_{\mathbf{y}_t \sim \pi_\theta(\cdot | \mathbf{x}, \mathbf{y}_{<t})} \pi_\theta(v | \mathbf{x}, \mathbf{y}_{<t}) \hat{A}_t \\ &\approx -\pi_\theta(v | \mathbf{x}, \mathbf{y}_{<t}) \hat{A}_t \end{aligned} \quad (14)$$

Similarly, substituting Eq. (13) into Eq. (11) yields the gradient when token  $v$  is sampled:

$$\begin{aligned}
\frac{\partial \mathcal{J}(\theta)}{\partial z_v} &= \frac{\mathbb{E}_{\mathbf{y}_t \sim \pi_\theta(\cdot | \mathbf{x}, \mathbf{y}_{<t})} \partial \pi_\theta(\mathbf{y}_t | \mathbf{x}, \mathbf{y}_{<t}) \hat{A}_t}{\pi_\theta(\mathbf{y}_t | \mathbf{x}, \mathbf{y}_{<t}) \partial z_v} \\
&= \mathbb{E}_{\mathbf{y}_t \sim \pi_\theta(\cdot | \mathbf{x}, \mathbf{y}_{<t})} (1 - \pi_\theta(\mathbf{y}_t | \mathbf{x}, \mathbf{y}_{<t})) \hat{A}_t \quad (15) \\
&= \mathbb{E}_{\mathbf{y}_t \sim \pi_\theta(\cdot | \mathbf{x}, \mathbf{y}_{<t})} (1 - \pi_\theta(v | \mathbf{x}, \mathbf{y}_{<t})) \hat{A}_t \\
&\approx (1 - \pi_\theta(v | \mathbf{x}, \mathbf{y}_{<t})) \hat{A}_t
\end{aligned}$$